Supporting data

Hydrogen production via alcohol oxidation using mixed conductive graphene oxide membrane reactor

Toma Kiyozawa,[a] Kotaro Furuya,[a] Mana Yamaguchi,[a] Ami Takase,[a] Shintaro Ida,[b] Muhammad Sohail Ahmad[b*], Tetsuya Kida[a,b*]

[a]*Department of Applied Chemistry and Biochemistry, Graduate School of Science and Technology, Kumamoto University, Kumamoto 860-8555, Japan*
[b]*Institute of Industrial Nanomaterials (IINa), Kumamoto University, 2-39-1 Kurokami, Chuo-ku, Kumamoto 860-8555 Japan*

Corresponding Author
Muhammad Sohail Ahmad
E-mail: sohail@kumamoto-u.ac.jp
Tetsuya Kida
E-mail: tetsuya@kumamoto-u.ac.jp

Graphene oxide synthesis

Expanded graphite (3.0 g, Ito Graphite, Kuwana, Japan), potassium permanganate (18 g, Fujifilm Wako), sulfuric acid (360 mL, Fujifilm Wako), and phosphoric acid (40 mL, Fujifilm Wako) were mixed in a beaker. The mixture was heated in an oil bath at 50 ± 2 °C for 14 hours with continuous stirring. After heating and stirring, the mixture was cooled to room temperature, and 400 mL of ice was added, followed by the addition of hydrogen peroxide (Fujifilm Wako) until the solution turned yellow-orange. The resulting solution was centrifuged at 5000 rpm for 15 minutes, and the precipitate was washed three times with 5% HCl (Fujifilm Wako) and three times with distilled water. The washed graphite oxide dispersion was then subjected to ultrasonic treatment for 12 hours to exfoliate the layered graphite oxide into monolayer GO. Finally, the dispersion was centrifuged at 10000 rpm for 15 minutes, and the supernatant was collected to obtain the GO dispersion.

Fabrication of the GO membrane

GO membranes were prepared by vacuum filtration of a GO dispersion. For the fabrication of Ce-doped GO (Ce-GO) membranes, $Ce(SO_4)_2 \cdot 4H_2O$ (Fujifilm Wako) was added to a GO suspension at a ratio of 0.0050 mmol per 20 mg of GO. The mixture was thoroughly stirred before being subjected to a vacuum filtration. During the filtration process, a 0.4 μm pore size filter paper (Merck Millipore) was used, supported by two additional layers of filter paper with a pore size of 180 μm (Merck Millipore) placed underneath. To obtain a partially reduced Ce-GO (Ce-prGO) membrane, the Ce-GO membrane was thermally treated in an incubator (MD-100, Yonezawa). The thermal reduction was performed in air at 120 °C for 25 min.

Characterizations

The interlayer distance of GO nanosheets was investigated by X-ray diffraction (MiniFlex 600, Rigaku, Tokyo, Japan) using CuKα radiation ($\lambda = 0.154$ nm, 40 kV, 15 mA) over a 2θ range of 2°–80°. The structural features of the GO membranes were examined by Raman spectroscopy with a 532 nm excitation source (NRS-3100, Jasco, Easton, MD, USA). Surface oxygen functionalities were identified by X-ray photoelectron spectroscopy (Theta Probe, Thermo Fisher Scientific, Waltham, MA, USA). The surface functional groups of the membranes were studied using Fourier transform infrared

spectrometer (FTIR 4100, JASCO). Finally, the microstructures of membranes incorporating catalyst layers were characterized using scanning electron microscopy (SU8000, Hitachi).

Gas permeation studies

Gas permeation experiments were performed at 25 °C under atmospheric pressure using a teflon cell, in which the prepared membrane was placed in the cell, as shown in Fig. S3. The feed and permeate gas flow rates were controlled at 100 mL/min, respectively, with mass flow controllers (Horiba). On the feed side, humidified H_2 (30%) - He (30%) in Ar was supplied, while humidified Ar was introduced on the permeate side. Humidification was achieved by bubbling the gases through distilled water, and the relative humidity was maintained at 90% as measured by a humidity sensor.

To regulate operating temperature, the gas permeation membranes were placed in an incubator. The permeate gases (H_2 and He) were analyzed with a gas chromatograph equipped with a thermal conductivity detector (GC-8A, Shimadzu, Kyoto, Japan).

The permeation flux of H_2 was calculated using the following equation:

$$J_{H_2} = \frac{C_{H_2} \times V_{total}}{S} \quad \text{(S-1)}$$

Where J_{H2} is the H_2 permeation flux (mL/cm^2/min), CH_2 is the H_2 concentration in the permeate gas, $Vtotal$ is the total permeate gas flow rate (mL/min), and S is the effective membrane area (cm^2).

Hydrogen production studies

Hydrogen production experiments via alcohol oxidation were performed using Ce-prGO membranes, which exhibit excellent mixed proton–electron conductivity and hydrogen separation capability. The Ce-prGO membrane, coated with Pt/C catalyst on both sides, was assembled within a Teflon cell (as illustrated in Fig. S6). Prior to the reaction, the membrane was humidified by flowing argon gas bubbled through deionized water on both the feed and sweep sides for 1.5 hours. Subsequently, the feed side was supplied with argon gas bubbled through a 20 vol% aqueous alcohol solution (or specified concentration) at a flow rate of 100 mL min^{-1}, while the sweep side received dry argon at the same rate. The effluent gas from the sweep side was analyzed using gas chromatography equipped with a thermal conductivity detector (GC-TCD, GC-8A, Shimadzu).

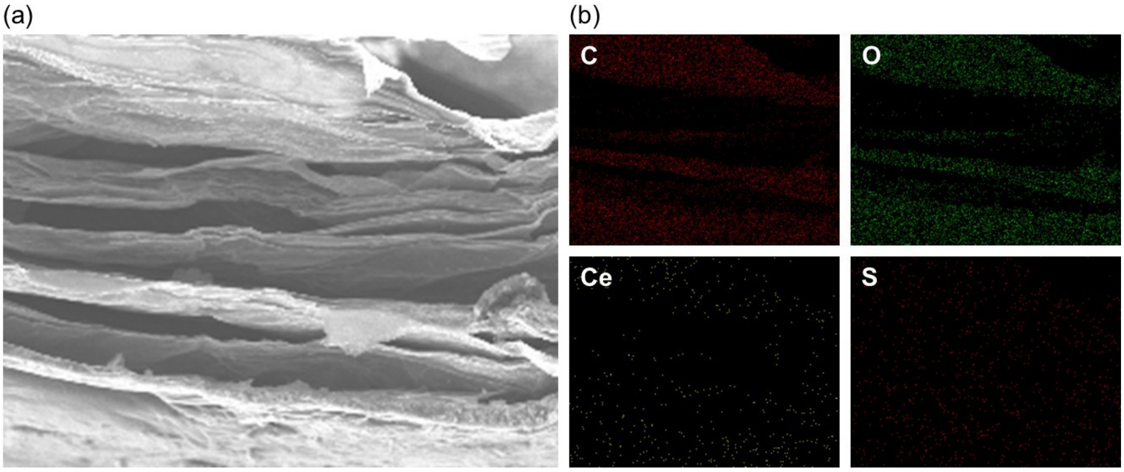

Fig. S1 (a) Cross-sectional SEM image of the layered material. Corresponding EDX elemental mapping showing the distribution of carbon (C), oxygen (O), cerium (Ce), and sulfur (S).

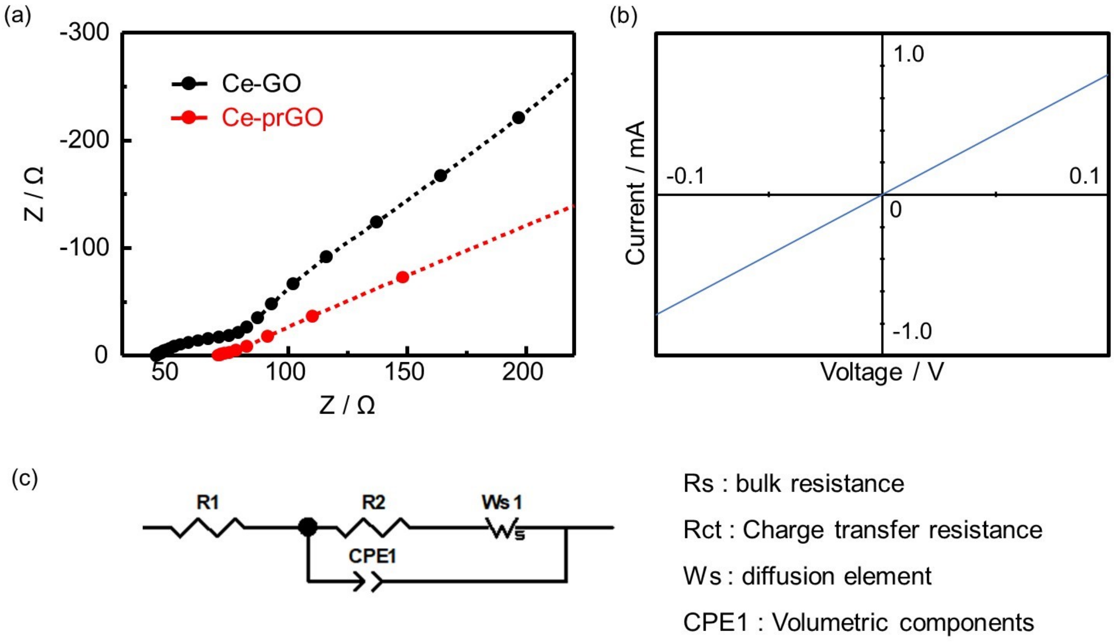

Fig. S2. Nyquist plots for Ce-GO and Ce-prGO electrodes. (b) The linear relationship between current and voltage for the Ce-prGO material. (c) The equivalent electrical circuit used to model the impedance data, with definitions for the circuit components.

.

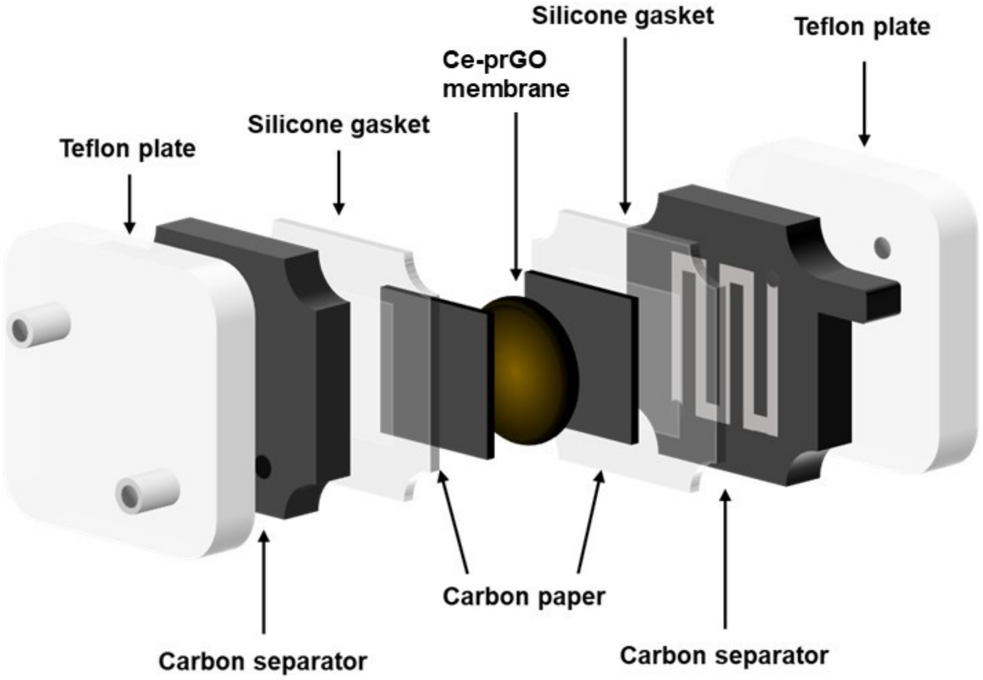

Fig. S3. Reactor setup for the gas separation, using graphene-based membrane

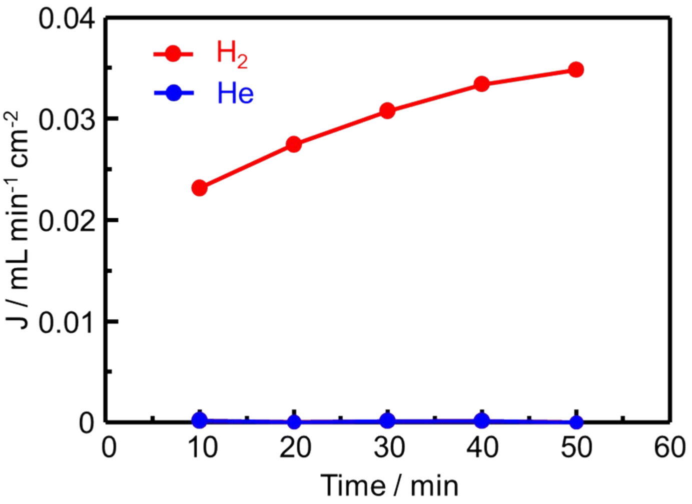

Fig. S4. Gas permeance of H_2 and He through the Ce-prGO membrane, shows selective permeation of H_2 at room temperature.

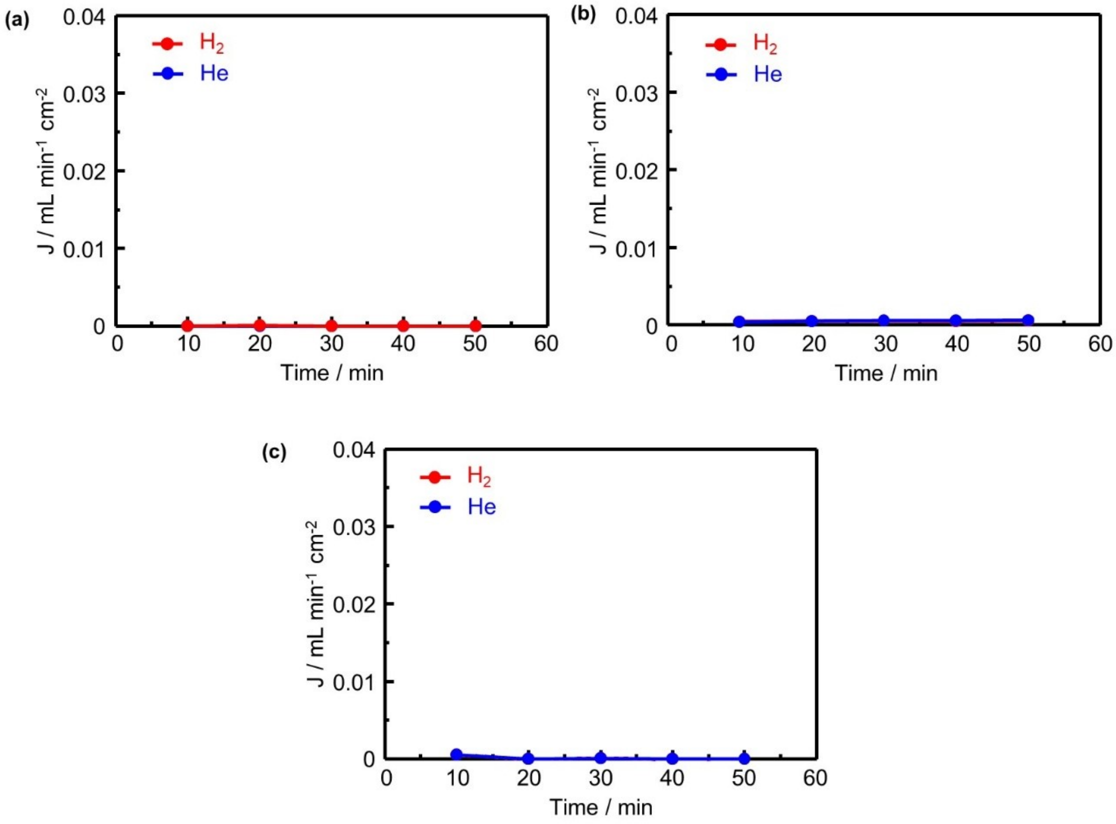

Fig. S5. Gas permeance of H_2 and He, under different conditions, at room temperature (a) using Ce-GO membrane, (b) membrane under dry conditions (no humidity), (c) membrane without catalyst coating

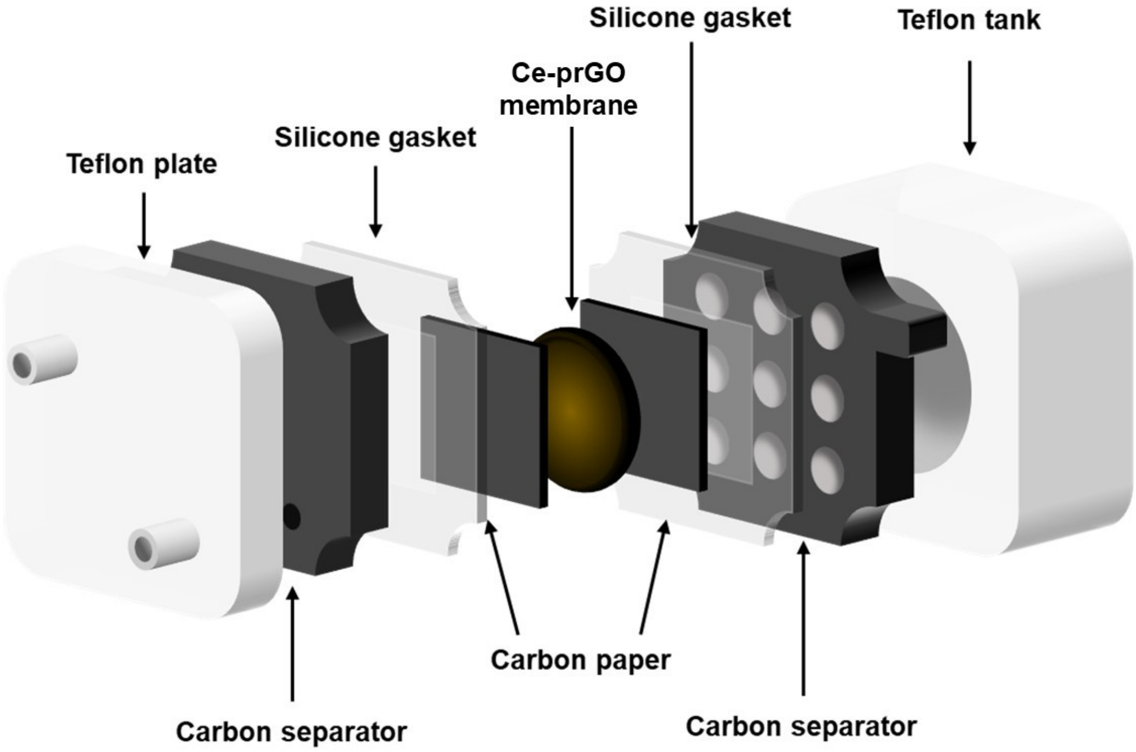

Fig. S6. The reactor setup of the hydrogen production from alcohol solutions experiments.

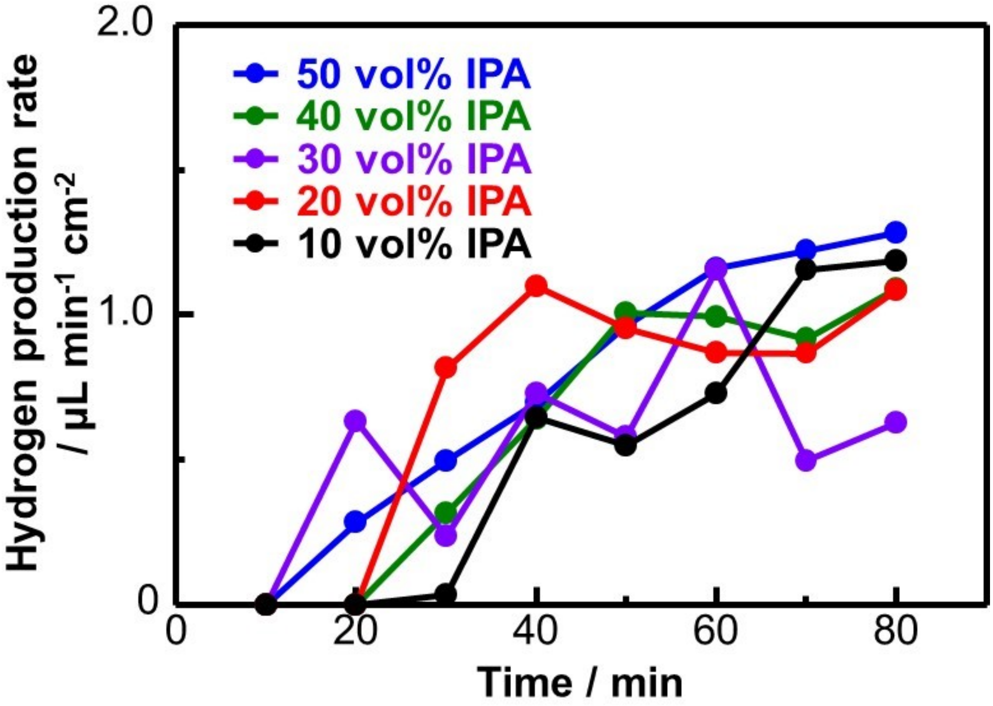

Fig. S7. Hydrogen production rate using Ce-prGO membrane over time at various concentrations of isopropanol 10 vol %, 20, 30, 40 and 50 vol% at room temperature.

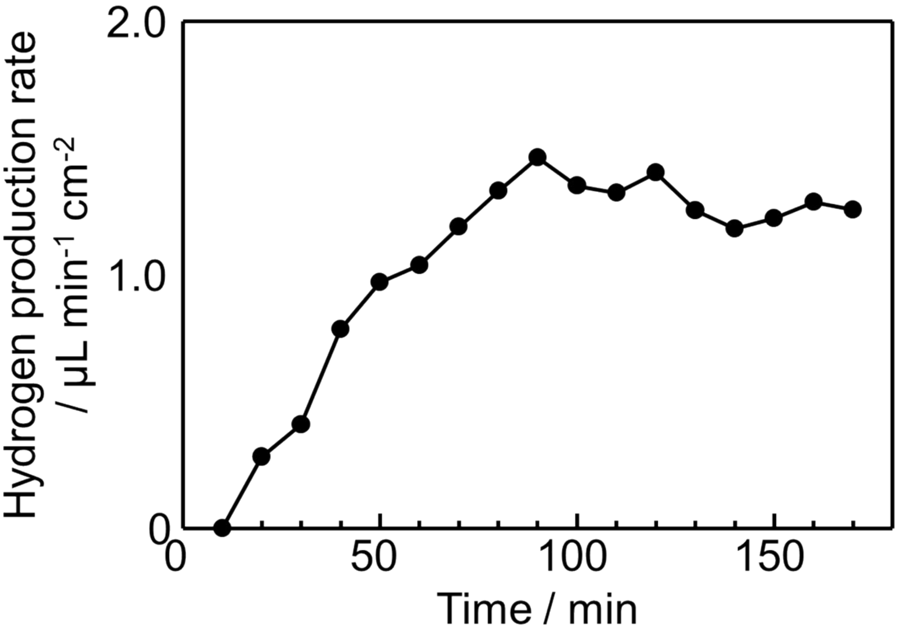

Fig. S8. Operational stability test: Cumulative hydrogen production volume over a prolonged duration (3 hrs) using the Ce-prGO membrane reactor with a 50 vol% aqueous isopropanol solution. The stable production rate confirms the robustness of the Pt Ce-prGO system.

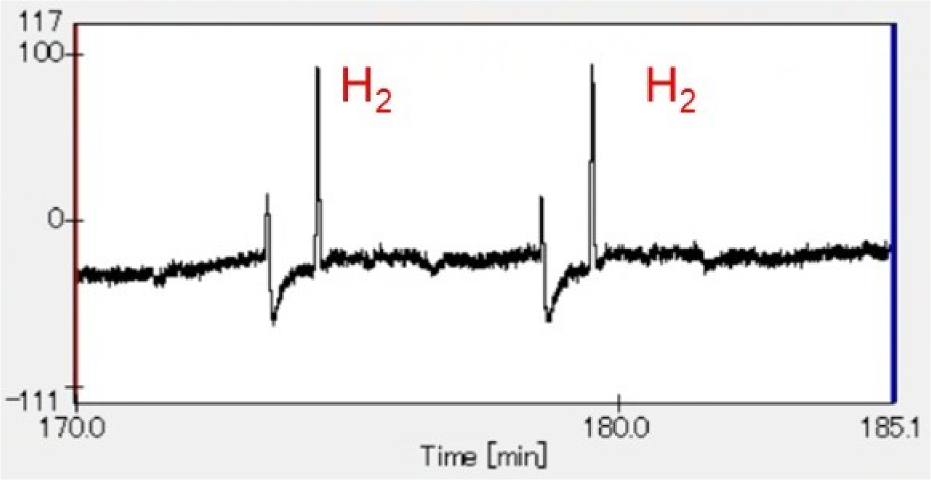

Fig. S9. Gas chromatography, chromatogram of the product gas collected at the final stage of the prolonged operation experiment (3hrs). The absence of the single corresponding to CO_2, or CO within the detection limits provides conclusive evidence for the production of CO_2-free hydrogen in the Ce-prGO membrane reactor.

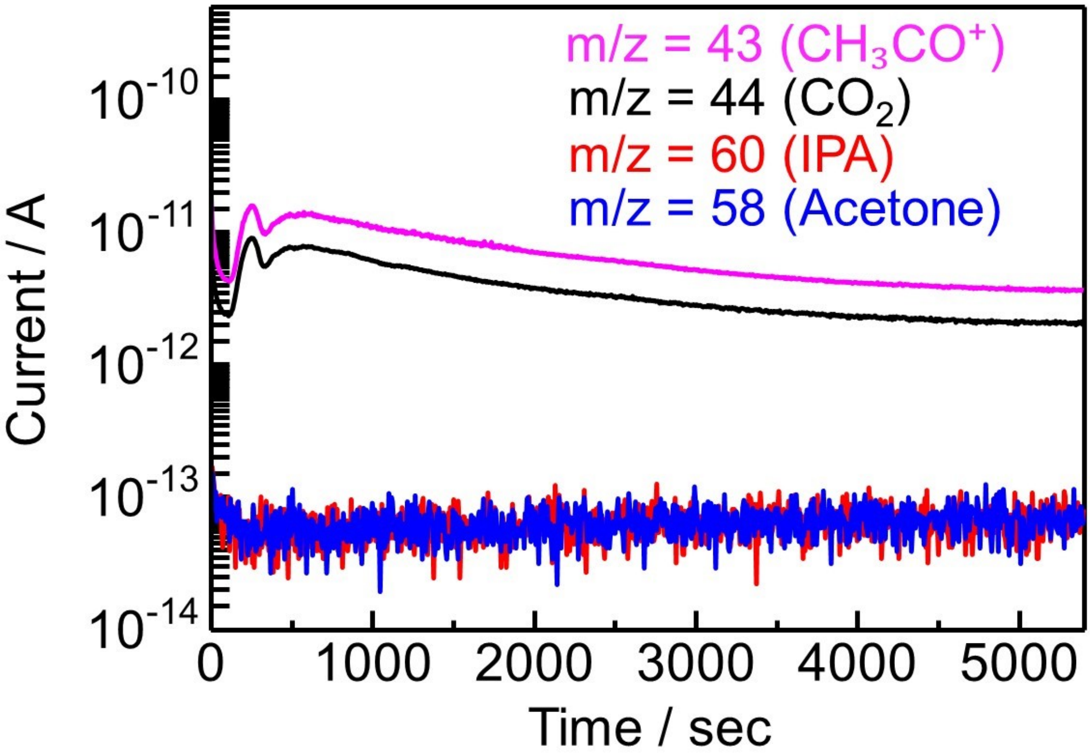

Fig. S10. Mass spectrum analysis of the gas phase products swept by Argon over a 50 vol% aqueous isopropanol solution. The detection of the acetyl cation m/z 43 confirms the oxidation of isopropanol to acetone on the feed side of the membrane reactor.

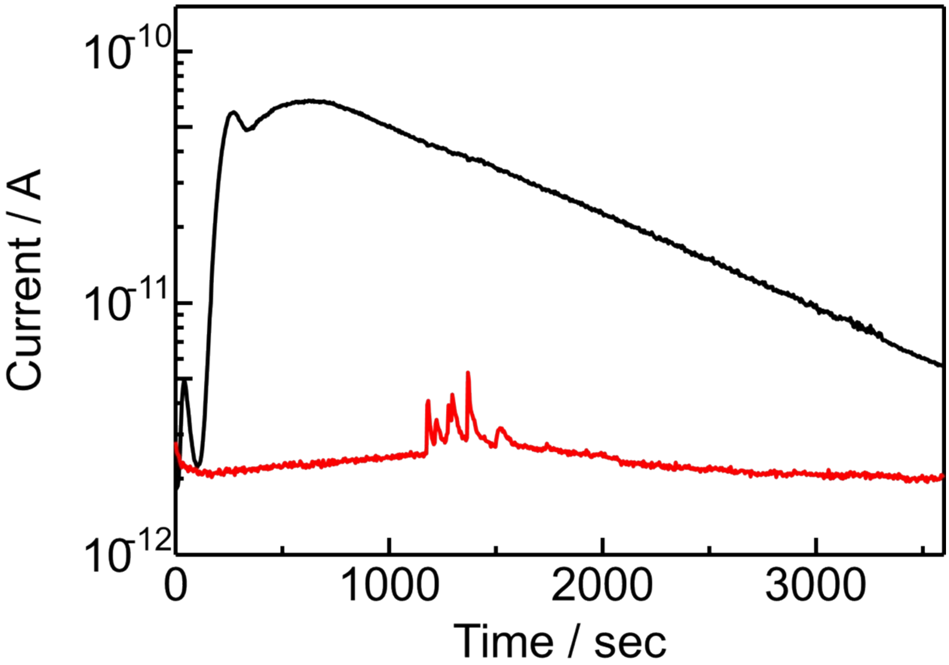

Fig. S11. Mass spectrum (MS) analysis of the gas product generated from the feed side containing deuterium-labeled alcohol (methanol-$_4$). The detection of D_2 (m/z 4) (black line) provides direct evidence that proton abstraction during alcohol oxidation is the source of the hydrogen produced.

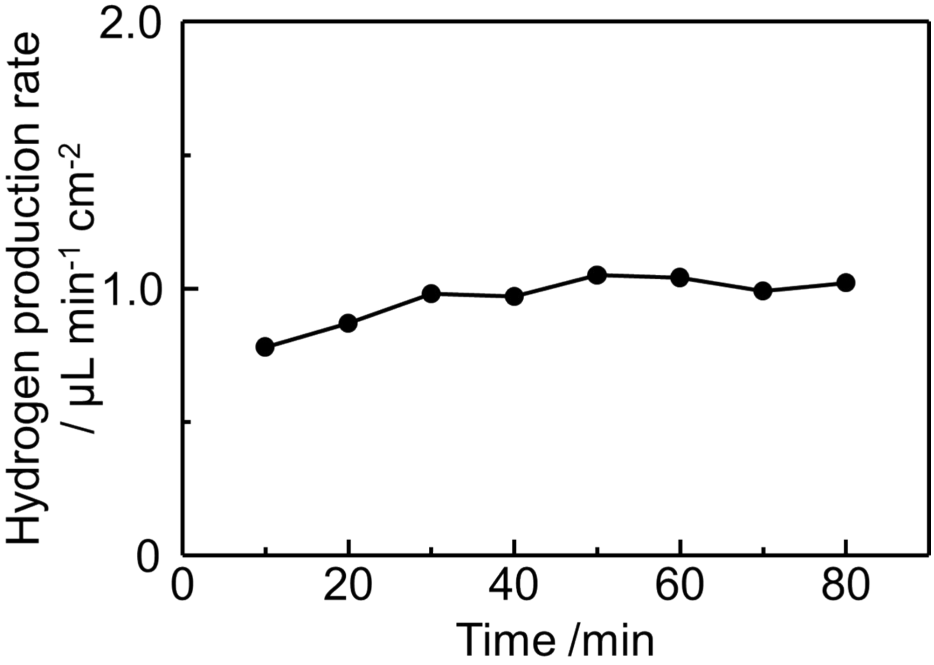

Fig S12. Control experiment demonstrating the effect of dissolved oxygen, hydrogen production using a 50 vol% aqueous isopropanol solution with the prior removal of dissolved oxygen (via Ar purging). The accelerated onset of H_2 generation in the purged solution confirms that residual O_2 competes as an electron acceptor.